THE JOURNAL OF PHYSICAL CHEMISTRY B

ARTICLE

pubs.acs.org/JPCB

Peculiar Thermodynamics of the Second Critical Point in Supercooled Water

C. E. Bertrand and M. A. Anisimov*

Institute for Physical Science & Technology and Department of Chemical & Biomolecular Engineering, University of Maryland, College Park, Maryland 20742, United States

ABSTRACT: On the basis of the principle of critical-point universality, we examine the peculiar thermodynamics of the liquid−liquid critical point in supercooled water. We show that the liquid−liquid criticality in water represents a special kind of critical behavior in fluids, intermediate between two limiting cases: the lattice gas, commonly used to model liquid−vapor transitions, and the lattice liquid, a weakly compressible liquid with an entropy-driven phase separation. While the ordering field in the lattice gas is associated with the chemical potential and the order parameter with the density, in the lattice liquid the ordering field is the temperature and the order parameter is the entropy. The behavior of supercooled water is much closer to lattice-liquid behavior than to lattice-gas behavior. Using new experimental data recently obtained by Mishima [J. Chem. Phys. 2010, 133, 144503], we have revised the parametric scaled equation of state, previously suggested by Fuentevilla and Anisimov [Phys. Rev. Lett. 2006, 97, 195702], and obtain a consistent description of the thermodynamic anomalies of supercooled water by adjusting linear backgrounds, one critical amplitude, and the critical pressure. We also show how the lattice-liquid description affects the finite-size scaling description of supercooled water in confined media.

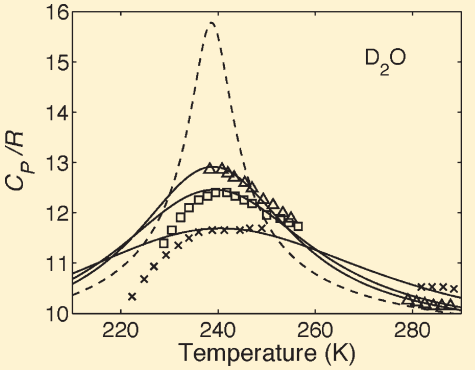

INTRODUCTION

In 1971, Voronel[1] speculated that the liquid state of some substances might be envisioned as a state between two singularities, the gas−liquid critical point and the absolute stability limit of the liquid phase located below the triple-point temperature (see also ref 2, p 387). Calorimetric measurements in water[3] indeed showed a noticeable increase of the isobaric heat capacity upon modest supercooling (∼−8 °C). However, the definitive breakthrough in this field came with Angell et al.'s publication in 1973[4] of accurate heat-capacity measurements of supercooled water emulsified in heptane, made using a procedure developed by Rasmussen and MacKenzie.[5] Reaching temperatures as low as −39 °C at atmospheric pressure, Angell and co-workers[6,7] observed a sharp increase in the isobaric heat capacity that resembles a critical-point-like singularity. In subsequent experiments, the isothermal compressibility[8,9] and thermal expansivity[10,11] were also found to exhibit similar anomalies upon supercooling.

A plausible, thermodynamically consistent, explanation of the global phase behavior of supercooled water was formulated in 1992 by Poole et al.[12] According to these authors there exists a critical point of liquid−liquid coexistence, deep in the supercooled region, which terminates a line of first-order transitions between two liquid phases, namely, a low-density liquid and a high-density liquid. Consequently, the observed anomalies in the heat capacity, compressibility, and thermal expansivity result from the "virtual" divergence of density and entropy fluctuations at this critical point. The hypothesis of a second critical point is supported by simulations of realistic models of water[13−22] and by various water-like models.[23−28] Although the simulation data yield a variety of critical pressure values, most find it somewhere in the range between 100 and 350 MPa; however, the possibility of a negative critical pressure has also been proposed.[14,15] Additionally, experimental data for H_2O and D_2O are consistent with the existence of a liquid−liquid critical point in the supercooled region.[29−32] On the basis of the melting curve of metastable ice IV, Mishima and Stanley[29] have estimated that the location of the LLCP in water is at approximately 100 MPa and 220 K.

The existence of the liquid−liquid critical point (LLCP) in metastable water is not the only thermodynamically consistent explanation of water's anomalies. Three additional scenarios, which do not imply the existence of a LLCP, have also been proposed: the stability-limit (SL) scenario,[34] the singularity-free (SF) scenario,[35,36] and the critical-point free (CPF) scenario.[37] Recently, Stokely et al.[28] have shown, for a water-like lattice model, how all four scenarios can be described by varying two quantities, the strength of the hydrogen bonds and the cooperativity of the hydrogen bonds. The CPF and SL scenarios are realized in the limit of high cooperativity and weak strength of the hydrogen bonds, the SF scenario corresponds to the absence of

Special Issue: H. Eugene Stanley Festschrift

Received: April 29, 2011
Published: June 10, 2011

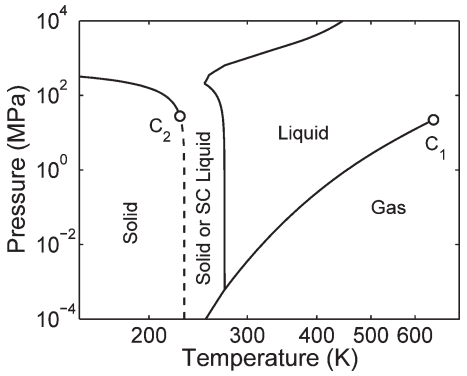

Figure 1. Phase diagram for water with vapor−liquid (C1) and liquid−liquid (C2) critical points. Solid curves show vapor−liquid, liquid−liquid, and liquid−solid phase transitions;[39] the dashed curve is the Widom line. The liquid−liquid transition line is adopted from Mishima;[32] the location of the liquid−liquid critical point (P_c = 27.5 MPa and T_c = 227.4 K) is estimated in this work. "SC" stands for "supercooled".

cooperativity, and the LLCP scenario is expected when both features are present. A realistic estimate of the corresponding contributions to the free energy of water shows a preference for the LLCP scenario and locates the critical point at a positive pressure.[28]

To coordinate the various experimental findings, Fuentevilla and Anisimov[33,38] developed a scaled parametric equation of state for the neighborhood of the liquid−liquid critical point in supercooled water. It was assumed that the liquid−liquid transition in supercooled water does exist and is characterized by a scalar order parameter and thus belongs to the Ising-model universality class. The particular microscopic nature of the order parameter is not essential for a phenomenological description; however, it is important to distinguish between systems with long-ranged intermolecular interactions and systems with short-ranged interactions. For systems with long-ranged interactions, the fluctuations of the order parameter do not affect the equation of state. For such systems the equation of state can be formulated in a mean-field approximation that does not depend on the universality class. Correlating the available experimental data via the parametric equation of state, Fuentevilla and Anisimov located the critical point at about 232 K and 27 MPa; the latter is much lower than expected from computer simulations. In Figure 1, we show the phase diagram of water[39] and the LLCP with the critical parameters, 27.5 MPa and 227 K, which we have obtained in this work and consider to be more reliable. Mishima[32] has recently obtained qualitative agreement between his extensive data on the volume of supercooled water as a function of temperature and pressure and the Fuentevilla-Anisimov parametric equation of state. In particular, Mishima has located the LLCP at about 40 MPa and 225 K for H_2O.

Recent experiments on water confined in nanopores[40−44] allow for the suppression of crystallization such that properties can be measured in the "no-man's land" across the Widom line below the critical pressure or across the liquid−liquid separation line above the critical pressure as shown in Figure 1. In particular, because the heat capacity passes through a maximum and the expansivity passes through a minimum at the expected Widom-line temperature, these data provide indirect evidence in favor of the LLCP scenario. However, because the properties in confined conditions are, generally, different from those in the bulk, depending on the confined geometry and on the specific interaction with the surface, these experiments should be treated specially.

In this paper we examine the peculiar thermodynamics of the liquid−liquid critical point in supercooled water. We show that the liquid−liquid criticality in water represents a special kind of critical behavior in fluids, intermediate between two limiting cases: the lattice gas, commonly used to model gas−liquid transitions, and the lattice liquid, a weakly compressible liquid with an entropy-driven phase separation. While in the lattice gas the ordering field is associated with the chemical potential and the order parameter with the density, in the lattice liquid the ordering field is associated with the temperature and the order parameter with the entropy. The behavior of supercooled water appears to be much closer to the lattice-liquid behavior than to the lattice-gas behavior. Using the new information on the liquid−liquid transition line recently suggested by Mishima,[32] we have revisited and revised the parametric scaled equation of state earlier proposed by Fuentevilla and Anisimov.[38] We show that all available response functions (the heat capacity, compressibility, and expansivity) of supercooled ordinary and heavy water can be consistently described by the lattice-liquid scaled equation of state by adjusting only linear backgrounds, one critical amplitude, and the critical pressure. The optimal value of the critical pressure is virtually the same as that predicted by Fuentevilla and Anisimov; however, the critical temperature is lower by ∼5 K. We also show how this peculiar thermodynamics affects the finite-size scaling description of supercooled water in porous media. In particular, we explain the fact emphasized by Nagoe et al.[44] that the temperature of maximum heat capacity is practically independent of pore size.

LATTICE GAS VERSUS LATTICE LIQUID

Lattice Gas. The lattice-gas model is a symmetric prototype of the liquid−vapor transition in fluids, which, despite its simplicity, reflects the most important features of fluid phase behavior.[45] The lattice-gas model is equivalent to the Ising model for incompressible anisotropic ferromagnets. All fluids, including water, belong to the same universality class of criticality as the Ising model.[46,47] Criticality in the lattice-gas/Ising model is described by two independent scaling fields h_1 and h_2—designated ordering field and thermal field, respectively—and a third field $h_3(h_1,h_2)$, which is the critical part of the field-dependent thermodynamic potential. The independent scaling fields are thermodynamically conjugate to two scaling densities. The strongly fluctuating scaling density φ_1 (the order parameter) is conjugate to h_1 and the weakly fluctuating scaling density φ_2 is conjugate to h_2. The scaling fields and densities are therefore related by

$$dh_3 = \varphi_1 dh_1 + \varphi_2 dh_2 \quad (1)$$

The critical point is defined by $h_1 = h_2 = h_3 = 0$.

In scaling theory, the thermodynamic potential h_3 is a homogeneous function of h_1 and h_2.[46] Asymptotically

$$h_3 = |h_2|^{2-\alpha} f^{\pm}\left(\frac{h_1}{|h_2|^{2-\alpha-\beta}}\right) \quad (2)$$

where $f^{\pm}$ is a scaling function and the superscript ± refers to $h_2 > 0$ and $h_2 < 0$, respectively. The form of the scaling function is

universal; however, it contains two thermodynamically independent (but system-dependent) amplitudes which are related to all other asymptotic amplitudes by universal relations. The critical exponents α and β are universal within the Ising class of critical-point universality.

For $h_1 = 0$ and $h_2 > 0$, there is a single phase characterized by $\varphi_1 = 0$ and

$$\varphi_2 = \left(\frac{\partial h_3}{\partial h_2}\right)_{h_1} = \frac{A_0^+}{1-\alpha}|h_2|^{1-\alpha} \quad (3)$$

For $h_1 = 0$ and $h_2 < 0$, there are two coexisting phases with

$$\varphi_1 = \left(\frac{\partial h_3}{\partial h_1}\right)_{h_2} = \pm B_0|h_2|^{\beta} \quad (4)$$

and

$$\varphi_2 = -\frac{A_0^-}{1-\alpha}|h_2|^{1-\alpha} \quad (5)$$

While the superscript $\pm$ refers to the states at $h_2 > 0$ and $h_2 < 0$, the prefactor $\pm$ in eq 4 refers to the branches of the order parameter on the $h_1 > 0$ and $h_1 < 0$ sides, respectively. In the above expressions $\alpha \simeq 0.109$ and $\beta \simeq 0.326$ are universal critical exponents,[48] and $A_0^{\pm}$ and B_0 are nonuniversal amplitudes. In eqs 3 and 5, we have neglected a fluctuation-induced analytic contribution to the scaling density φ_2,[49,50] which has been absorbed into the noncritical background terms in our analysis.

There are three scaling susceptibilities, "strong" $\chi_1 = (\partial\varphi_1/\partial h_1)_{h_2}$, "weak" $\chi_2 = (\partial\varphi_2/\partial h_2)_{h_1}$, and "cross" $\chi_{12} = (\partial\varphi_1/\partial h_2)_{h_1} = \chi_{21} = (\partial\varphi_2/\partial h_1)_{h_2}$. Asymptotically and in zero ordering field, $h_1 = 0$:

$$\chi_1 = \Gamma_0^{\pm}|h_2|^{-\gamma} \quad (6)$$

$$\chi_2 = A_0^{\pm}|h_2|^{-\alpha} \quad (7)$$

$$\chi_{12} = -\beta B_0|h_2|^{\beta-1}\ (h_2 < 0)\quad \chi_{12} = 0\ (h_2 > 0) \quad (8)$$

where the critical exponent $\gamma = 2 - \alpha - 2\beta \simeq 1.239$[48] and the Ising critical amplitude $\Gamma_0^{\pm}$ is related to B_0 and $A_0^{\pm}$ through the universal ratios, $\alpha\Gamma_0^+A_0^+/B_0^2 \simeq 0.0581$, $\Gamma_0^+/\Gamma_0^- \simeq 4.8$, and $A_0^+/A_0^- \simeq 0.523$.[51]

In one-component fluids the physical fields are the pressure P, the temperature T, and the chemical potential μ; μ is conjugate to the physical density ρ, while the temperature is conjugate to the entropy density $s = \rho S$ (S is the entropy per molecule). It is convenient to introduce dimensionless variables by defining

$$\hat{T} = \frac{T}{T_c}\quad \hat{P} = \frac{P}{\rho_c k_B T_c}\quad \hat{\mu} = \frac{\mu}{k_B T_c} \quad (9)$$

and

$$\hat{\rho} = \frac{\rho}{\rho_c}\quad \hat{s} = \hat{\rho}\frac{S}{k_B} \quad (10)$$

where k_B is Boltzmann's constant. Here and in what follows, a subscript "c" denotes a quantity taken at the critical point. In addition, we define

$$\Delta\hat{T} = \frac{T-T_c}{T_c}\quad \Delta\hat{P} = \frac{P-P_c}{\rho_c k_B T_c}\quad \Delta\hat{\mu} = \frac{\mu-\mu_c}{k_B T_c} \quad (11)$$

and

$$\Delta\hat{\rho} = \frac{\rho-\rho_c}{\rho_c}\quad \Delta\hat{s} = \frac{s-s_c}{\rho_c k_B} \quad (12)$$

The physical fields and densities are thermodynamically related by

$$d\hat{P} = \hat{\rho}\,d\hat{\mu} + \hat{s}\,d\hat{T} \quad (13)$$

The lattice-gas model establishes the relationship between the physical fields and the scaling fields via the mapping

$$h_1 = \Delta\hat{\mu} + a\Delta\hat{T} \quad (14)$$

$$h_2 = \Delta\hat{T} \quad (15)$$

$$h_3 = \Delta\hat{P} - \Delta\hat{\mu} - \hat{s}_c\Delta\hat{T} \quad (16)$$

This mapping implies that $\Delta\hat{\rho} = \varphi_1$ and $\Delta\hat{s} = \varphi_2 + a\varphi_1$. The lattice gas therefore shares the symmetry of the Ising model under the transformation $\Delta\hat{\rho} \rightarrow -\Delta\hat{\rho}$.

There is a subtlety in the equivalence of the Ising model and the lattice gas. In classical thermodynamics, the critical values of the chemical potential and the entropy are arbitrary and thus can be adopted on the basis of convenience. In particular, there are two practical choices for $\hat{s}_c$: $\hat{s}_c = (d\hat{P}/d\hat{T})_c$ and $\hat{s}_c = 0$. For the first choice, as follows from eq 13, the coefficient $a = 0$ and $\varphi_2 = \Delta\hat{s}$. This choice represents the purely Ising-model case: the density of entropy is not linearly coupled with the order parameter and thus it is the weakly fluctuating density. For the second choice, $a = -(d\hat{P}/d\hat{T})_c$, the slope of the chemical potential at $h_1 = 0$ follows the slope of the pressure along the phase coexistence, and the density of entropy couples with the molecular density through the coefficient a. For both choices, the order parameter remains associated with the density, $\varphi_1 = \Delta\hat{\rho}$.

In general, real fluids do not have the symmetry of the lattice-gas model because their properties are not symmetric with respect to the sign of $\Delta\hat{\rho}$. To account for this asymmetry, the theory of "complete scaling", developed by Fisher and co-workers,[52,53] proposes that the scaling fields are analytic functions of all physical fields: the chemical potential $\Delta\hat{\mu}$, the temperature $\Delta\hat{T}$, and the pressure $\Delta\hat{P}$. As shown by Wang and Anisimov[54,55] the contribution from the pressure mixing into h_1 and h_2 is significant only for highly asymmetric fluids, such as high-molecular-weight hydrocarbons, electrolytes, and polymer solutions, and thus unimportant for the further discussion of liquid−liquid criticality in weakly compressible supercooled water. A simplified version of complete scaling, which ignores the pressure contribution, known as "revised scaling",[56] expresses the scaling fields through the physical fields as

$$h_1 = \Delta\hat{\mu} + a\Delta\hat{T} \quad (17)$$

$$h_2 = \Delta\hat{T} + b\Delta\hat{\mu} \quad (18)$$

$$h_3 = \Delta\hat{P} - \Delta\hat{\mu} - \hat{s}_c\Delta\hat{T} \quad (19)$$

In the revised-scaling formulation, the liquid−gas asymmetry is controlled by the system-dependent coefficient b. The order parameter in the asymmetric fluid, $\varphi_1 = \Delta\hat{\rho} - b\Delta\hat{s}$, contains contributions from the density and from the density of entropy.

Lattice Liquid. Two features make the second critical point in water phenomenologically different from the well-known gas−liquid critical point. The negative slope of the liquid−liquid phase transition line in the $P-T$ plane means that high-density liquid water is the phase with larger entropy. The relatively large value of this slope at the critical point (about 25 times greater

than for the gas−liquid transition at the critical point) indicates the significance of the entropy change relative to the density change and, correspondingly, the importance of the entropy fluctuations. Second, supercooled water tends to separate upon pressurizing. These features suggest that liquid−liquid phase separation in water is mostly driven by entropy rather than by energy.

To apply the language of Ising criticality to a weakly compressible single-component liquid that exhibits a liquid−liquid phase transition, we consider the following model. Let the system be described by the Ising scaling fields such that the temperature $\Delta\hat{T}$ is taken to be the dominant contribution to h_1, and $\Delta\hat{\mu}$ is taken to be the dominant contribution to h_2. Additionally, we consider the case where phase separation occurs for increasing chemical potential, which increases with the pressure. With a particular choice of the critical entropy, $\hat{s}_c = 0$, the relations between the Ising scaling fields and physical fields now read

$$h_1 = \Delta\hat{T} + a'\Delta\hat{\mu} \tag{20}$$

$$h_2 = -\Delta\hat{\mu} + b'\Delta\hat{T} \tag{21}$$

$$h_3 = \Delta\hat{P} - \Delta\hat{\mu} \tag{22}$$

where a' and b' are taken to be asymmetry coefficients, with a' representing the slope $-\mathrm{d}\hat{T}/\mathrm{d}\hat{P}$ along the liquid−liquid transition line ($h_1 = 0$) taken at the critical point. In this case, the entropy density and the molecular density are given by

$$\Delta\hat{s} = \varphi_1 + b'\varphi_2 \quad \Delta\hat{\rho} = -\varphi_2 + a'\varphi_1 \tag{23}$$

If $b' \ll 1$ and $a' \ll 1$, the entropy density makes the major contribution to the order parameter.

From the relationships between the physical and scaling fields, given by eqs 20−22, one can derive the critical parts, designated by a subscript "cr", of the physical response functions, namely, the isothermal compressibility κ_T, isobaric thermal expansivity α_P, and the isobaric heat capacity C_P, which are related to linear combinations of the scaling susceptibilities by

$$(\hat{\rho}^2\hat{\kappa}_T)_{\mathrm{cr}} = \left(\frac{\partial\hat{\rho}}{\partial\hat{\mu}}\right)_{T,\mathrm{cr}} = \chi_2 - 2a'\chi_{12} + (a')^2\chi_1 \tag{24}$$

$$(\hat{\rho}\hat{\alpha}_P)_{\mathrm{cr}} = -\left(\frac{\partial\hat{\rho}}{\partial\hat{T}}\right)_{P,\mathrm{cr}} = (1-a'b')\chi_{12} - a'\chi_1 + b'\chi_2 + \hat{S}(\hat{\rho}^2\hat{\kappa}_T)_{\mathrm{cr}} \tag{25}$$

$$\left(\hat{\rho}\frac{\hat{C}_P}{\hat{T}}\right)_{\mathrm{cr}} = \left(\hat{\rho}\frac{\partial\hat{S}}{\partial\hat{T}}\right)_{P,\mathrm{cr}} = \chi_1 + 2b'\chi_{12} + (b')^2\chi_2 + 2\hat{S}(\hat{\rho}\hat{\alpha}_P)_{\mathrm{cr}} - \hat{S}^2(\hat{\rho}^2\hat{\kappa}_T)_{\mathrm{cr}} \tag{26}$$

where the reduced entropy per molecule is $\hat{S} = (\hat{s}_c + \varphi_1 + b'\varphi_2)/(1 - \varphi_2 + a'\varphi_1)$. These expressions reduce to the relations used in the previous scaling analysis made by Fuentevilla and Anisimov[38] in the approximation $\hat{S} \simeq 0$, which corresponds to $\Delta\hat{\mu} \simeq \Delta\hat{P}$ and $\Delta\hat{\rho} \simeq -\Delta\hat{V}$. The more general revised-scaling expressions for the critical parts of the physical response functions, which include all mixing coefficients are presented in Appendix A. The full physical susceptibilities, i.e., the quantities measured in experiments, include background contributions, $(\hat{\rho}^2\hat{\kappa}_T)_b$, $(\hat{\rho}\hat{\alpha}_P)_b$, and $(\hat{\rho}\hat{C}_P/\hat{T})_b$, which are assumed to be regular functions of pressure and temperature. For example,

$$\left(\frac{\partial\hat{\rho}}{\partial\hat{\mu}}\right)_T = (\hat{\rho}^2\hat{\kappa}_T)_{\mathrm{cr}} + (\hat{\rho}^2\hat{\kappa}_T)_b \tag{27}$$

Just as the Ising model represents the symmetric limit ($a \to 0$, $b \to 0$) of eqs 17−19, we can define a "lattice liquid" as the system corresponding to the symmetric limit ($a' \to 0$, $b' \to 0$) of the transformations eqs 20−22. Our model is purely phenomenological; the term "lattice liquid" is used loosely and does not imply that the liquid has a lattice structure. In the lattice liquid, the entropy density is the order parameter and the molecular density is the weakly fluctuating density:

$$\Delta\hat{s} = \varphi_1 \quad \Delta\hat{\rho} = -\varphi_2 \tag{28}$$

Hence, the ordering field is $\Delta\hat{T}$ and the thermal field is $-\Delta\hat{\mu}$. The phase diagram of a symmetric lattice liquid is different from the phase diagram of a lattice gas: the liquid−liquid transition line is perfectly vertical in the $\mu - T$ plane, at $T = T_c$, and phase separation occurs when μ reaches μ_c. As the critical value of the chemical potential is arbitrary, one can adopt $\mu_c = 0$. Although the lattice-liquid and the lattice-gas scaling properties exhibit the same universal critical behavior, the power laws for the corresponding physical properties are markedly different. For example, along the critical isotherm ($\Delta\hat{T} = 0$) in the one-phase region ($\Delta\hat{\mu} < 0$), the density of the lattice liquid scales as

$$\Delta\hat{\rho} \sim |\Delta\hat{\mu}|^{1-\alpha} \tag{29}$$

with $1 - \alpha \simeq 0.89$. Along the same thermodynamic path, the lattice-gas density scales as

$$\Delta\hat{\rho} \sim |\Delta\hat{\mu}|^{1/\delta} \tag{30}$$

where $1/\delta \simeq 0.21$ is related to the other universal critical exponents through $\beta(\delta - 1) = \gamma$. Further scaling relationships for the lattice liquid can be found by substituting the definitions of the lattice-liquid scaling fields into the general scaling expressions. Several of the resulting relations are presented in Appendix B.

Two-State Model for the Lattice Liquid. We will now develop a phenomenological mean-field model that clarifies the nature of the order parameter in a polyamorphic single-component liquid and which shares the scaling properties of the lattice liquid. The model is a version of the popular "two fluid states" model,[57,58] which traces its lineage back to a 19th century paper by Röntgen.[59] Relatively recently, Ponyatovskii et al.[60] and, more quantitatively, Moynihan[61] have nicely described the emergence of a LLCP in supercooled water as resulting from the effects of nonideality in a mixture of two "components", the concentration of which is controlled by thermodynamic equilibrium. However, while Moynihan assumed a "regular-solution" type of nonideality, which implies an energy-driven phase separation, we assume an "athermal-solution" type of nonideality. This leads to purely entropy-driven phase separation. The scaling properties of these two models are essentially different. The "regular-solution" version describes the lattice-gas type of the phase diagram while the "athermal-solution" versions predicts lattice-liquid behavior.

Let us assume that the liquid is a "mixture" of two states, A and B, of the same molecular species. For instance, these two states could represent two different arrangements of the hydrogen-bond network in water.[62] We also assume that the individual molecules are identical in both states, leaving aside any concerns

regarding the continuity of the fluid phases.[63] The concentration of water molecules involved in either structure, denoted x for state A and $1 - x$ for state B, is controlled by the "chemical reaction"

$$\mathrm{A} \rightleftharpoons \mathrm{B} \tag{31}$$

Following Monynihan,[61] we assume that the reaction is endothermic; i.e., the equilibrium is shifted toward the formation of state A state if the temperature decreases. Unlike a binary fluid, the concentration x is not an independent variable but is determined as a function of pressure P and temperature T from the condition of thermodynamic equilibrium.

The chemical potential (Gibbs energy per molecule) can be separated into two parts corresponding to the contributions from the specific chemical potentials, μ_A and μ_B, associated with each state:

$$\mu = \mu_A x + \mu_B(1 - x) \tag{32}$$

Hence, the field conjugate to the concentration x is the difference between the chemical potentials $\mu_{AB} = \mu_A - \mu_B$. This change in the Gibbs energy of reaction, μ_{AB}, is related to the chemical equilibrium constant, $K = K(T)$, by[64]

$$\ln K = \frac{\mu_{AB}}{k_B T} \tag{33}$$

Now we postulate an equation of state for this model that produces the phase diagram of a lattice liquid. The chemical potential $\mu(P,T)$, taken relative to its arbitrary critical value μ_c, is given by

$$\frac{\mu - \mu_c}{k_B T} = \frac{\Delta\mu}{k_B T} = x \ln x + (1 - x)\ln(1 - x) + \omega x(1 - x) \tag{34}$$

where the interaction parameter ω is assumed to be independent of temperature but may depend on pressure. This equation of state, known as the "athermal solution model",[65] predicts symmetric liquid−liquid phase separation for any temperature, with critical concentration $x_c = 1/2$, if $\omega \geq 2$. Liquid-phase coexistence is found from the condition

$$\frac{\mu_{AB}}{k_B T} = \frac{\partial}{\partial x}\left(\frac{\Delta\mu}{k_B T}\right)_P = \ln\frac{x}{1 - x} + \omega(1 - 2x) = 0 \tag{35}$$

and the stability limit is determined by

$$\frac{\partial^2}{\partial x^2}\left(\frac{\Delta\mu}{k_B T}\right)_P = \frac{1}{x(1 - x)} - 2\omega = 0 \tag{36}$$

If the interaction parameter increases with pressure as

$$\omega = \omega_0(\hat{P}_c + \Delta\hat{P} + \ldots) \tag{37}$$

separation into two fluid phases with different equilibrium values of x will occur above the critical pressure $\hat{P}_c = \omega_c/\omega_0$, where ω_c is the critical interaction parameter. Thus, the liquid−liquid critical point for the athermal solution corresponds to $\omega = \omega_c = 2$ and $x_c = 1/2$. The liquid−liquid separation in this model is driven only by the nonideal entropy of mixing.

However, unlike an athermal nonideal binary fluid, the entropy-driven phase separation in a polyamorphic single-component liquid does not happen at any temperature. Contrarily, the critical temperature T_c is specified through the temperature dependence of the reaction equilibrium constant K by

$$\ln K = -\frac{\lambda}{k_B}\left(\frac{1}{T} - \frac{1}{T_c}\right) \simeq \frac{\lambda}{k_B T}\Delta\hat{T} \tag{38}$$

where λ is the heat (enthalpy change) of reaction, which is assumed to be independent of temperature. By definition, $K = 1$ and $\mu_A = \mu_B$ at the critical temperature.

Expanding μ_{AB} in the vicinity of the critical point in powers of $\Delta\hat{P}$ and $\Delta\hat{x} = (x - x_c)/x_c$ and combining eqs 33 and 38, we obtain at lowest order

$$\Delta\hat{T} \simeq \frac{1}{\hat{\lambda}}\left[-\omega_0\Delta\hat{P}\Delta\hat{x} + \frac{2}{3}(\Delta\hat{x})^3\right] \tag{39}$$

where $\hat{\lambda} = \lambda/k_B T_c$. To establish a connection between this result and the symmetric lattice-liquid model, we will consider the mean-field Landau expansion[64] of the ordering field given by

$$h_1(h_2,\varphi_1) = a_0 h_2\varphi_1 + \frac{u_0}{6}\varphi_1^3 \tag{40}$$

where a_0 and u_0 are system dependent constants. When combined with the symmetric lattice-liquid ($a' \to 0$, $b' \to 0$) transformations eqs 20−22, this becomes

$$h_1 = \Delta\hat{T} = -a_0\Delta\hat{\mu}\Delta\hat{s} + \frac{u_0}{6}(\Delta\hat{s})^3 \tag{41}$$

Comparing the above equation to eq 39, we conclude that the order parameter, $\varphi_1 = \Delta\hat{s}$, introduced in the previous section for the lattice liquid is related to the concentration of state A in the two-fluid model by

$$\Delta\hat{s} \simeq \hat{\lambda}\Delta x \tag{42}$$

with $a_0 = \omega_0/\hat{\lambda}^2$ and $u_0 = 4/\hat{\lambda}^4$. Other results for the lattice-liquid model based on the mean-field Landau expansion are presented in Appendix C.

To make the connection between our model and the lattice liquid more precise, the chemical potential $\Delta\hat{\mu}$, which in eq 41 plays the role of the "weak field", can be expressed through the pressure $\Delta\hat{P}$ in linear approximation as

$$\Delta\hat{\mu} = \Delta\hat{P} - \hat{s}_c\Delta\hat{T} \tag{43}$$

In zero field $h_1 = 0$, $\Delta\hat{T} = 0$, and $\Delta\hat{\mu} = \Delta\hat{P}$ for any choice of the critical value of entropy $\hat{s}_c$. In nonzero field, this approximation is exact only for $\hat{s}_c = 0$. The difference leads to a higher-order term $\sim(\Delta\hat{s})^4$ in eq 41 that can be neglected in the lowest approximation.

A finite slope of liquid−liquid coexistence in the $P-T$ plane can be incorporated into the two-state lattice-liquid model if one assumes that the Gibbs energy change of the reaction also depends on pressure, such that

$$\frac{\mu_{AB}}{k_B T} \simeq \hat{\lambda}\Delta\hat{T} + \hat{\kappa}\Delta\hat{P} \tag{44}$$

The physical meaning of the constant $\hat{\kappa}$ follows from the relation

$$\hat{\kappa} \simeq \left(\frac{\partial(\hat{\mu}_{AB})}{\partial\hat{P}}\right)_T = -\frac{1}{\hat{\rho}^2}\left(\frac{\partial\hat{\rho}}{\partial x}\right)_P \simeq -\frac{\hat{\lambda}}{\hat{\rho}^2}\left(\frac{\partial\hat{\rho}}{\partial\hat{s}}\right)_P \tag{45}$$

It follows from eq 23, with $b' = 0$, that

$$\frac{1}{\hat{\rho}^2}\left(\frac{\partial\hat{\rho}}{\partial\hat{s}}\right)_P = a' = -\frac{d\hat{T}}{d\hat{P}} \tag{46}$$

dx.doi.org/10.1021/jp204011z | J. Phys. Chem. B 2011, 115, 14099–14111

In this approximation the constant $\hat{\kappa}$ is proportional to the volume change of reaction, namely, $\hat{\kappa} = \hat{\lambda}(d\hat{T}/d\hat{P})$. Therefore, while for the purely symmetric lattice liquid, with the vertical slope of the liquid−liquid coexistence in $P-T$ space, the entropy and the density follow eq 28, the finite $P-T$ slope generates the difference in the densities of coexisting phases, while the entropy remains the only contribution to the order parameter and the scaling field $h_2 = -\Delta\hat{P}$ is the same as in the symmetric lattice liquid.

A further asymmetric correction to the two-fluid model, a nonzero value of the mixing coefficient b' in eq 23, breaks the athermal-solution nature of the model and mixes it with some features of the lattice-gas model, including an energetic contribution into the phase separation. The temperature term in the scaling field h_2 may significantly affect the shape of the liquid−liquid coexistence curve. Real water undoubtedly possesses features of both models; however, as our following analysis shows, the lattice-liquid model captures the important anomalous features of supercooled water's behavior.

SCALING DESCRIPTION OF BULK THERMODYNAMIC PROPERTIES

In this section, we describe the available experimental data on ordinary and heavy water in the supercooled region with the lattice-liquid scaling model. The description of the data is similar to, but more self-consistent than, that reported by Fuentevila and Anisimov[38] for ordinary water and by Fuentevilla[33] for heavy water. It also contains fewer system-dependent parameters and is theoretically more accurate.

The simplest scaled parametric equation of state is known as the "linear model" (LM).[49,50,66] Rather than the scaling fields h_1 and h_2, the LM is most conveniently expressed in terms of the " polar" variables r, which is a measure of the absolute distance from the critical point, and θ, which is a measure of angular position in the h_1-h_2 plane. The explicit relationships between the variables (h_1, h_2, φ_1) and (r, θ) are

$$h_1 = ar^{\beta+\gamma}\theta(1-\theta^2) \tag{47}$$

$$h_2 = r(1-b^2\theta^2) \tag{48}$$

$$\varphi_1 = kr^{\beta}\theta \tag{49}$$

where a and k are system-dependent amplitudes and $b^2 = (\gamma - 2\beta)/\gamma(1-2\beta) \simeq 1.36$ is a universal constant. Notably, the scaling properties are analytic functions of θ. In the $\varepsilon = 4 - d$ expansion of renormalization-group theory,[46] where d is the spatial dimensionality, the LM matches the Ising equation of state exactly to order ε^2.[67] More accurate scaled parametric equations of state such as the "cubic model", for which $\varphi_1 = kr^{\beta}\theta(1 + c\theta^2)$, do not yield substantially different results but have been shown to match the Ising equation of state to order ε^3.[68] The singular part of the thermodynamic potential is given by

$$h_3 = -akr^{2-\alpha}f(\theta) + h_1\varphi_1 \tag{50}$$

where, on the basis of the values of the $d = 3$ Ising critical exponents, $f(\theta) \simeq -0.592 + 2.02\theta^2 - 1.59\theta^4$. The weakly fluctuating scaling density derived from this equation of state is

$$\varphi_2 = akr^{1-\alpha}s(\theta) \tag{51}$$

where $s(\theta) \simeq 1.12 - 1.97\theta^2$. The scaling susceptibilities are given by

$$\chi_1 = \frac{k}{a}r^{-\gamma}c_1(\theta) \tag{52}$$

$$\chi_{12} = kr^{\beta-1}c_{12}(\theta) \tag{53}$$

$$\chi_2 = akr^{-\alpha}c_2(\theta) \tag{54}$$

where the functions $c(\theta)$ are[50,49]

$$c_0(\theta) = 1 - 0.104\theta^2 - 0.177\theta^4 \tag{55}$$

$$c_1(\theta) = (1 - 0.476\theta^2)/c_0(\theta) \tag{56}$$

$$c_{12}(\theta) = -\theta(1.24 - 0.59\theta^2)/c_0(\theta) \tag{57}$$

$$c_2(\theta) = (0.995 + 1.43\theta^2 - 0.907\theta^4)/c_0(\theta) \tag{58}$$

Following Fuentevilla and Anisimov,[38] we reduce the number of system-dependent parameters, on the basis of results from the Ising model with short-range interactions,[69] by assuming $k/a = 1$. In ref 38 the parametric expression for χ_2 was empirically modified to remove the effects of fluctuations far from the critical point by letting $\chi_2 = ak(r^{-\alpha} - 1)c_2(\theta)$. This change was intended to imitate the fluctuation-induced analytic background B_{cr} in the weak susceptibility along the path $h_1 = 0$. Because this procedure was only applied to the weak susceptibility, thermodynamic consistency was compromised in this point. Instead, in this work, we retain the original asymptotic form of χ_2 as given by eq 52 and absorb all possible nonasymptotic contributions, including B_{cr}, into adjustable backgrounds, $(\hat{\rho}^2\hat{\kappa}_T)_b$, $(\hat{\rho}\hat{\alpha}_P)_b$, and $(\hat{\rho}\hat{C}_P/\hat{T})_b$, where the density is calculated using eq 23.

Locating the path $h_1 = 0$ is an important step in the application of the scaling model to the description of experimental data. This path defines liquid−liquid coexistence above the critical pressure and the "Widom line", the line of χ_1 maxima, in the one-phase region (below the critical pressure). We have adopted an equation for the liquid−liquid coexistence curve from a recent publication of Mishima,[32] namely,

$$T = 231.4 - 0.1478P - 0.0003399P^2 \tag{59}$$

with T in K and P in MPa and have assumed that this equation describes the Widom line when extrapolated into the one-phase region. Equation 59 predicts the value of the coexistence slope in the $P-T$ plane at the critical point, a', as a function of P_c, because the path $h_1 = 0$ is curved in $P-T$ space. In particular, for $P_c = 27.5$ MPa, $a' = 0.074$. Fuentevilla and Anisimov incorporated this curvature by adding a term $\propto\Delta\hat{P}^2$ to the relationship between h_1 and $\Delta\hat{P}$. Additionally, in ref 38, a term $\propto\Delta\hat{T}$ (with a small coefficient $b' = a'$) was mixed into h_2 to account for asymmetry in this field with respect to a temperature change (see eq 21). Mishima,[32] in applying the parametric equation of state of Fuentevilla and Anisimov, adopted $b' = 1$, which produces a stronger contribution of $\Delta\hat{T}$ into h_2. In this work, we have found that neither of these additional terms are significant enough to improve the fit to the experimental data analyzed by us. Therefore, we use the linearized relations between the scaling fields and physical fields as given by eqs 20−22 with only one mixing

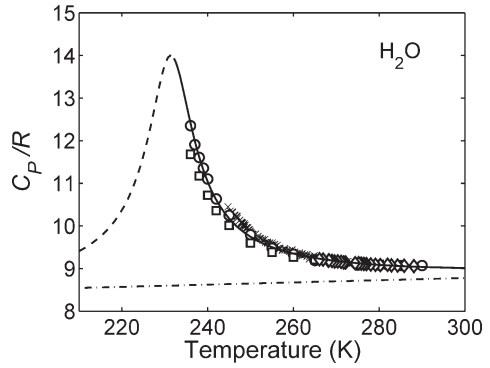

Figure 2. Isobaric heat-capacity experiments on H_2O (open circles,[7] crosses,[71] diamonds,[3] and squares[70]) and the prediction of the scaling parametric equation of state (solid curve in metastable region and dashed curve in unstable region). The estimated noncritical background is plotted as a dotted-dashed line.

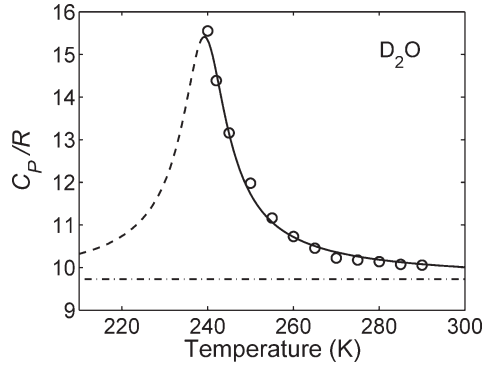

Figure 3. Isobaric heat-capacity experiments on D_2O (open circles[7]) and the prediction of the scaling parametric equation of state (solid curve in metastable region and dashed curve in unstable region). The estimated noncritical background is plotted as a dotted-dashed line.

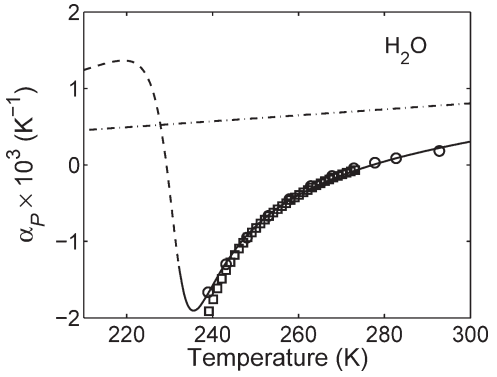

Figure 4. Thermal expansivity experimental data for H_2O at 0.1 MPa (open cirles[10] and squares[11]) and the prediction of the scaling parametric equation of state (solid curve in metastable region and dashed curve in unstable region). The estimated noncritical background is plotted as the dotted-dashed line.

coefficient a'. The adopted value $a' = 0.066$ is the effective slope of the Widom line at atmospheric pressure, which is slightly smaller than the slope at the critical pressure.

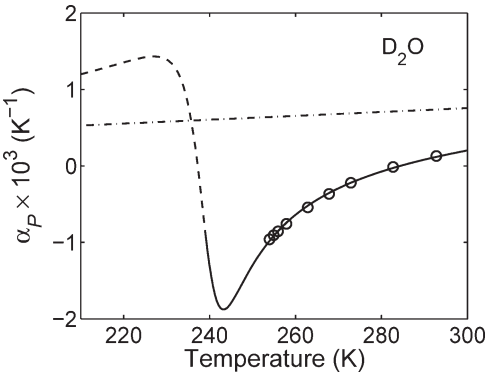

Figure 5. Thermal expansivity experimental data for D_2O at 0.1 MPa (open cirles[10]) and the prediction of the scaling parametric equation of state (solid curve in metastable region and dashed curve in unstable region). The estimated noncritical background is plotted as the dashed-dotted line.

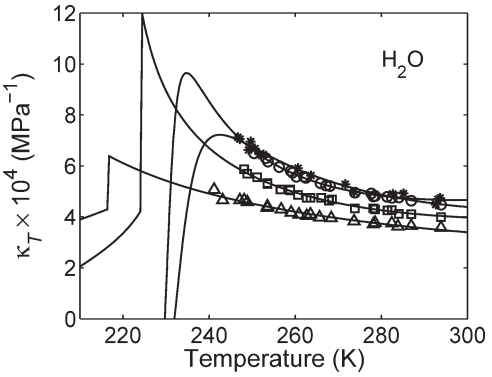

Figure 6. Isothermal compressibility experimental data for H_2O along isobars[8,9] (0.1 MPa (stars), 10 MPa (open circles), 50 MPa (squares), and 100 MPa (triangles)) compared with the scaling prediction at the same pressures (solid curves).

In describing the thermodynamic data for bulk supercooled water we adjust only one critical amplitude $k = a$, the critical pressure, and the backgrounds, which are assumed to be linear functions of temperature and pressure. By using linear backgrounds, we attribute all experimentally observed curvatures of the second thermodynamic derivatives to critical-point anomalies. To simplify the analysis we have used the approximation $\Delta\hat{\mu} \simeq \Delta\hat{P}$ in describing the data. In practice, the effects of this approximation may be absorbed by adjusting the linear backgrounds. There are at least three different sets of experimental heat-capacity data on deeply supercooled water shown in Figure 2: Angell and co-workers,[4,7] Tombari et al.,[71] and Archer and Carter.[70] As a compromise for fitting, we used the data of Angell and co-workers, which are located between those of Tombari et al. and Archer and Carter. Finally, the following experimental data for ordinary and heavy water have been used in the optimization: the isobaric-heat-capacity data obtained by Angell and co-workers[4,7] (Figures 2 and 3), the volumetric expansivity data by Hare and Sorensen[10] (Figures 4 and 5), and the isothermal compressibility data by Speedy and Angell,[9] Kano and Angell[8] (Figures 6 and 7), and Mishima[32] (Figure 8). For ordinary water, we have obtained $P_c = 27.5$ MPa and $T_c = 227.4$ K ($\rho_c = 0.97$ g/cm^3) for the location of the second critical

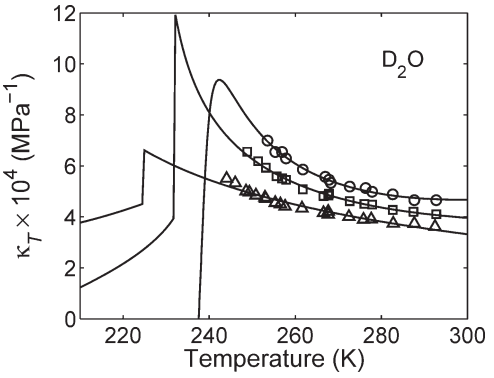

Figure 7. Isothermal compressibility experimental data for D_2O along isobars[8] (10 MPa (open circles), 50 MPa (squares), and 100 MPa (triangles)) compared with the scaling prediction at the same pressures (solid curves).

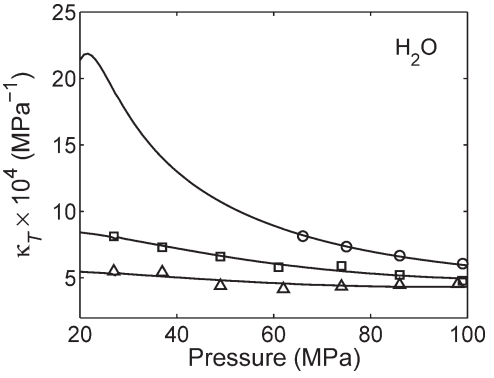

Figure 8. Isothermal compressibility experimental data for H_2O along isotherms[32] (230 K (open circles), 245 K (squares), and 260 K (triangles)) compared with the scaling prediction at the same temperatures (solid curves).

point. If eq 59 is used to calculate the critical temperature, rather than the linearized version used in our analysis, we find T_c = 227.1 K based on P_c = 27.5 MPa. Of particular note, we have confirmed the result of Fuentevilla and Anisimov that the critical pressure is much lower than that predicted by most simulations. The amplitude $k = a$ is found to be about 0.34, which is lower than the value $k = a \simeq 0.47$ reported in ref 38. This difference is due to the different treatments of the weak susceptibility χ_2, which contributes significantly into the isothermal compressibility and which is more accurate in the new description. The accuracy of these results will be considered in the Discussion. For the description of bulk heavy water, to minimize the number of adjustable parameters, we have adopted the same critical pressure P_c and amplitude k obtained for ordinary water but have let the critical temperature, found to be 235.2 K (ρ_c = 1.09 g/cm^3), and linear backgrounds differ. The results of the experimental-data analysis for ordinary and heavy water are presented in Figures 2−8 and Table 1.

We believe that the LLCP in supercooled water does not exhibit mean-field behavior. The mean-field version of the linear model can fairly describe the heat capacity and thermal expansivity with fit parameters k, P_c and linear background terms that differ from those used in the scaling optimization. However, the mean-field description always fails to adequately describe the compressibility anomaly.[72]

Table 1. Linear Backgrounds of Physical Susceptibilities

property	pressure (MPa)
$(\hat{C}_P)_b = 0.588\Delta\hat{T} + 8.585$	0.1
$(\kappa_T)_b = 9.808\Delta\hat{T} - 17.60$ [10^{-4} MPa^{-1}]	0.1
$(\kappa_T)_b = 12.15\Delta\hat{T} - 17.73$ [10^{-4} MPa^{-1}]	10
$(\kappa_T)_b = 7.305\Delta\hat{T} - 14.33$ [10^{-4} MPa^{-1}]	50
$(\kappa_T)_b = 2.431\Delta\hat{T} - 10.53$ [10^{-4} MPa^{-1}]	100
$(\alpha_P)_b = 0.892\Delta\hat{T} + 0.527$ [10^{-3} K^{-1}]	0.1

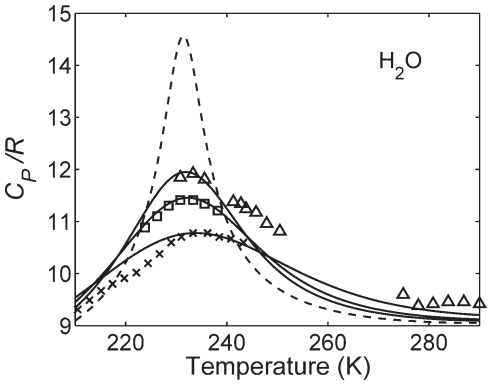

Figure 9. Isobaric heat-capacity experiments on confined H_2O[44] (2.3 nm (triangles), 2.1 nm (squares), 2.0 nm (crosses)) and the prediction based on the mean-field version of finite-size scaling. A mean-field prediction for the bulk heat capacity is plotted as a dashed curve, which fairly describes the experimental heat-capacity data with different values of the adjustable parameters.

FINITE-SIZE SCALING EFFECTS IN CONFINED WATER

Recent measurements of supercooled water in nanoporous media provide a unique means of testing features of the second-critical-point hypothesis. In confined water, spontaneous crystallization can be suppressed, allowing for measurements below the bulk homogeneous-nucleation temperature. Much recent attention has focused on dynamic properties of confined water, in particular the existence of a fragile-to-strong transition.[73] Additionally, several studies have investigated static properties of confined water.[41,43] Recently, Nagoe et al.[44] have reported a maximum in the isobaric heat capacity of normal and heavy water confined in cylindrical silica MCM-41 nanopores and have investigated the effect of changing pore diameter. Remarkably, the heat capacity exhibits a maximum in the near vicinity of the Widom line predicted for bulk water. In the bulk water, a maximum is predicted but not accessible because of spontaneous crystallization. However, the height of the maximum and the shape of the heat capacity in porous media differ significantly from those predicted in bulk water, as seen from Figures 9 and 10. It is known from the theory of finite-size scaling[74] that the behavior of near-critical systems in confined geometries deviates from that seen in bulk as a result of finite-size effects. To analyze these recent experiments in terms of critical phenomena, these finite-size effects need to be included.

Singular critical phenomena are only observed when the characteristic size of the system L is much larger than the

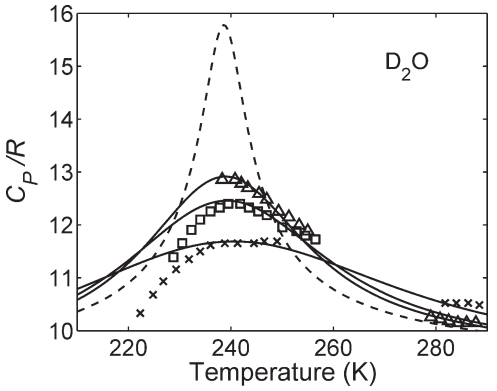

Figure 10. Isobaric heat-capacity experiments on confined D_2O[44] (2.4 nm (triangles), 2.1 nm (squares), 1.7 nm (crosses)) and the prediction based on the mean-field version of finite-size scaling. A mean-field prediction for the bulk heat capacity is plotted as a dashed curve, which fairly describes the experimental bulk heat-capacity data with different values of the adjustable parameters.

correlation length of critical fluctuations ξ. In systems where $L \sim \xi$, finite-size effects significantly alter the thermodynamic anomalies. In particular, singularities in the susceptibilities are replaced by L-dependent maxima, the location of these maxima is shifted relative to the bulk critical point, and the anomalous behavior is smeared out over a larger range of temperatures and pressures. Recent measurements of the correlation length in supercooled water suggest that ξ would reach ~1 nm near the Widom line at atmospheric pressure.[75] The nanopore diameters used by Nagoe et al. vary as $L \sim 1.7-2.4$ nm. These sizes are certainly in the range where finite-size effects will be relevant, if not dominant.

In general the finite-size susceptibilities are known to obey scaling laws. For example, the strong susceptibility scales as[76]

$$\chi_1(h_1,h_2;L) \approx L^{\gamma/\nu} P_1(h_1 L^{(\beta+\gamma)/\nu}, h_2 L^{1/\nu}) \qquad (60)$$

where ν is the correlation length exponent, which is defined in an isotropic system by[46]

$$\xi \approx \xi_0^{\pm} |h_2|^{-\nu} \qquad (h_1 = 0) \qquad (61)$$

where $\nu = 0.63$ for the $3d$ Ising universality class and $\xi_0^{\pm}$ is the correlation length amplitude for $h_2 > 0$ and $h_2 < 0$, respectively. In some special cases, namely $h_1 = 0$ and for a box geometry, the explicit form of the finite-size functions, such as P_1, have been calculated for the 3d Ising model.[77,78] The resulting predictions show excellent agreement with both experiments[79] and Monte Carlo simulations.[80] However, it is difficult to thoroughly analyze the existing data on supercooled water in terms of the existing theory of finite-size effects, because both $h_1 \neq 0$ and $h_2 \neq 0$ and the geometry of the silica MCM-41 nanopores is cylindrical. In the absence of an appropriate theory, we will focus on the qualitative features of finite-size effects. We note that the bulk heat-capacity data for ordinary and heavy water can be fairly well described by the mean-field version of the LM EOS (Figures 9 and 10). Therefore, for qualitative comparison, we will employ a mean-field treatment of finite-size effects that has the advantage that explicit calculations can be made for nonzero scaling fields, $h_1 \neq 0$ and $h_2 \neq 0$.

As an initial step toward a renormalization group calculation, Rudnick et al. have incorporated finite-size effects into a mean-field theory of critical phenomena.[77] In their theory, the critical part of the thermodynamic potential of a system confined to a box of side length L is given by

$$h_3(h_1,h_2) \simeq L^{-d} \ln\{\int d\varphi_0 \exp(-H_{mf})\} \qquad (62)$$

where H_{mf}, the mean-field Hamiltonian, is defined as

$$H_{mf}(h_1,h_2;\varphi_0) = L^d \left\{ \frac{1}{2} a_0 h_2 \varphi_0^2 + \frac{u_0}{4!} \varphi_0^4 - h_1 \varphi_0 \right\} \qquad (63)$$

Rudnick et al. assume that the fluctuation spectrum is restricted by the confining box but do not account for any additional surface effects. We have calculated the scaling susceptibilities χ_1, χ_2, and χ_{12} by taking derivatives of h_3 and evaluating the resulting integrals numerically. This mean-field theory reduces to the bulk theory in the limit $L \rightarrow \infty$. Although some care is required in defining the susceptibilities for $h_2 < 0$, this does not affect our analysis of the heat-capacity data, because $h_2 > 0$ for $P = 1$ atm. Anisimov et al.[50] have previously shown that the system-dependent coefficients a_0 and u_0 in eq 63 are related to the parameters of the mean-field version of the LM EOS by $a_0 = a/k$ and $u_0 = 3a/k^3$.

The predictions of the mean-field finite-size theory for normal and heavy water are presented in Figures 9 and 10. The calculations are based on values of $k = a$ and P_c found by fitting the mean-field version of LM EOS to the bulk heat-capacity data. Although the theoretical predictions do not follow the experimental points closely, they do capture all of the important features. In magnetic and fluid systems, finite-size scaling predicts a size-dependent shift in the temperature and pressure where physical properties exhibit a maximum, T_{max} and P_{max}, respectively. For the lattice liquid the roles of the fields h_1 and h_2 are essentially reversed relative to those of a lattice gas, making the temperature the ordering field h_1 and the presure the thermal field h_2. The Widom line, the line of maximum χ_1, is almost vertical in the $P-T$ plane (Figure 1) and hence the locations of C_P maxima are practically independent of the confinement. Thus the reported "very weak dependence of T_{max} on pore size" is completely consistent with the second-critical-point hypothesis, when finite-size effects are included. However, we expect a relatively large shift in the P_{max}, toward the two-phase region, similar to that seen for T_{max} in a lattice gas.[78] To within the experimental error, the curves for each substance are interrelated by finite-size scaling through a single dimensionless length scale L/ξ_0^+ with $\xi_0^+ = 0.7$ nm for H_2O and $\xi_0^+ = 0.64$ nm for D_2O. Finally, the theory predicts that the anomaly is smeared out above the transition temperature, although this effect appears to be more significant for the experimental data than for the predictions of mean-field finite-size scaling. That the smearing is greater for smaller size is best illustrated by the data for heavy water. At the maxima, the 2.4 nm pore heat capacity is greater than the 1.7 nm pore heat capacity but well below the bulk data.

DISCUSSION AND CONCLUSIONS

We have clarified the nature of the liquid−liquid critical point in supercooled water through the introduction of the "lattice-liquid" concept. While the near-critical behavior of a lattice liquid also belongs to the Ising universality class, it is markedly different

from that of the lattice gas, which belongs to the same universality class. Most importantly, the lattice-liquid order parameter, φ_1, is predominantly controlled by the entropy density, $\Delta\hat{s}$, and not the molar density, $\Delta\hat{\rho}$, as in the lattice gas. Hence the chemical potential $\Delta\hat{\mu}$ is the primary contribution to the "thermal" scaling field, h_2, as opposed to the temperature, $\Delta\hat{T}$. The physical origin of the lattice liquid's "peculiar" thermodynamic behavior is illuminated by a mean-field two-state model. This model assumes that a polyamorphic single-component liquid is composed of a "mixture" of two states of the same molecular species. The distinguishing feature of the lattice liquid is that the "chemical reaction" equilibrium between the two states is described by an "athermal solution model". This produces lattice-liquid type scaling behavior in the vicinity of the liquid−liquid critical point, whereas a "regular solution model" generates lattice-gas critical behavior. As discussed by Wang and Anisimov,[55] the relationships between the physical fields and the scaling fields are the same for the mean-field and scaling descriptions. Consequently, a mean-field model with lattice-liquid behavior can provide physical insight into the physical origins of the lattice-liquid scaling behavior. The mean-field description of a lattice liquid presented in this work is phenomenological; however, a microscopic model is needed to solidify the connection between this model and the physics of supercooled water. At this point, we do not know whether other suggested models, both mean-field[23] and microscopic,[28] of the liquid−liquid critical point, produce lattice-liquid or lattice-gas type criticality. The lattice-liquid description of criticality in supercooled water is remarkably similar to the scaling description of the transition between a molecular-liquid phase and an amorphous blue phase observed in some chiral liquids.[50] In particular, a mostly entropic order parameter and a temperature dominated ordering field are shared by these systems. We are led to speculate that other polyamorphic liquids might also be of the lattice liquid, rather than the lattice gas, type.

We have presented a significantly improved scaling description of the experimental data on supercooled water, the development of which was guided by the lattice-liquid concept and recent experiments of Mishima. The analysis of the physical susceptibilities (heat capacity, compressibility, and thermal expansivity) with our scaling description was made using only two free parameters, the amplitude coefficient k and the critical pressure P_c, and linear backgrounds. While the value of the critical pressure, $P_c \simeq 27.5$ MPa, has not shifted much from the previous findings of Fuentevilla and Anisimov ($P_c \simeq 27$ MPa), the critical temperature has lowered to the more feasible value $T_c = 227.4$ K. The particular value of the critical pressure significantly depends on which experimental data on the heat capacity are used for the analysis. For example, the value of the critical pressure found by fitting the heat-capacity data of Archer and Carter[70] is $P_c = 33.8$ MPa (with $k = 0.31$ and $T_c = 226.4$ K), whereas Tombari et al.'s data[71] lead to $P_c = 22.5$ MPa (with $k = 0.46$ and $T_c = 228.1$ K). The latter value is more consistent with the second set of experimental expansivity data reported by Hare and Sorensen[11] for which we find $P_c = 21.4$ MPa, $k = 0.35$, and $T_c = 228.25$ K. However, even with the uncertainty in the value of the critical pressure, our estimates for P_c are much lower than those based on recent simulations[18,22] ($P_c = 310$ and 135 MPa, respectively) and on experiments on confined water[40] ($P_c \simeq 160$ MPa). On the basis of possible uncertainties in the scaling description, we estimate the critical pressure to be lower than 40 MPa and higher than 20 MPa, and the corresponding critical temperature to be between 225 and 228 K. In terms of the recent model developed by Stokely et al.,[28] which reconciles the different scenarios for supercooled water by varying the values of two parameters, the hydrogen-bond strength and the cooperativity between hydrogen-bonds, a lower critical pressure corresponds to a greater contribution from bond cooperativity than previously suspected.

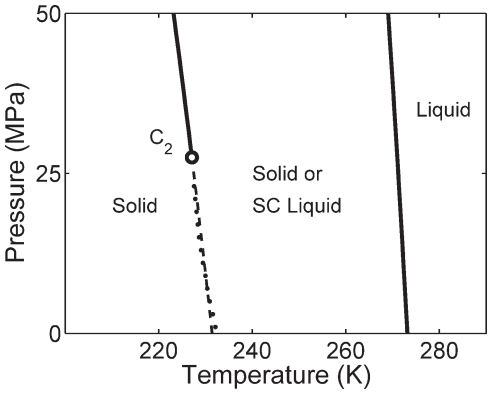

Figure 11. Estimated locus of the absolute stability limit of the supercooled liquid state (dots), which practically coincides with the Widom line (dashed line). The first-order transition lines are shown as the thick solid curves. "SC" stands for "supercooled".

Another important result of our analysis is the prediction on a thermodynamic instability in the one-phase region of supercooled water at temperatures corresponding to the Widom line. Our scaling description is thermodynamically stable for all temperatures and pressures, i.e., $(\kappa_T)_{cr} > 0$. However, when we include the linear background term $(\kappa_T)_b$ to fit the data, the scaling description predicts an instability at temperatures below the Widom line as can be seen from the apparent approach of the compressibility toward negative values in Figures 6 and 7. On the basis of a linear fit to the temperature and pressure dependence of the compressibility backgrounds, we have estimated the line of instabilities, which coincides with the Widom line fairly closely below the critical pressure, as is shown in Figure 11. We speculate that the predicted instability is not a pathology of the model but actually reflects the absolute stability limit of the supercooled liquid state. In this context we note that the line of spontaneous crystallization is located at slightly higher temperatures than the suggested Widom line.

We have applied a mean-field theory of finite-size scaling[77] to recent heat-capacity measurements in confined supercooled water.[44] The data are qualitatively consistent with three central features of the theory. The heat-capacity maximum is suppressed in proportion to a power of the confining length, the temperature at which the maximum is located does not shift much for the lattice liquid and the anomalous behavior of the heat capacity is smeared over a larger temperature range. We have applied the same mean-field theory to expansivity data derived from NMR measurements of water confined in MCM[42] (Figure 12). Because the bulk mean-field theory produces an unreasonably large expansivity below T_c, we have also plotted the bulk scaling behavior and the corresponding finite-size estimate based on eq 62. Notably, above T_c, the expansivity of confined water follows that of the bulk system almost exactly. This is in sharp contrast to the reduction in the maximum heat capacity seen in Figures 9 and 10 and remains unexplained.

Our application of the mean-field theory to porous media is only intended to demonstrate the feasibility of finite-size effects in the confined water system. There is certainly significant room

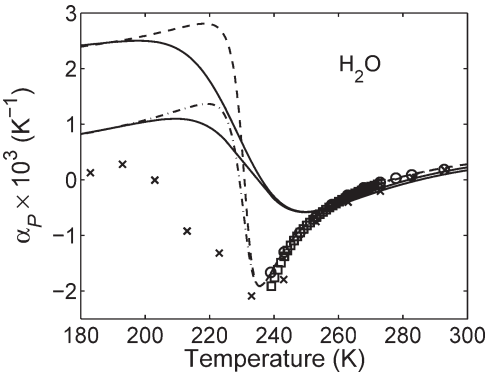

Figure 12. Thermal expansivity experimental data on confined H_2O at 0.1 MPa (crosses[42]) and on bulk water (open circles[10] and squares[11]) and the prediction based on the mean-field version of finite-size scaling. A mean-field prediction for the expansivity is plotted as a dashed curve, which fairly describes the experimental bulk expansivity data with other values of the adjustable parameters. The scaling prediction for the bulk expansivity, which differs significantly from the mean-field prediction below T_c, is shown as a dotted-dashed along with a finite-size prediction for this curve based on the mean-field theory.

for improvement with many aspects of the theory. A proper accounting of non-mean-field effects for the case $h_1 = 0$ would hopefully improve the quantitative agreement, as is the case for the 3*d* Ising model.[80] The geometry of the cylindrical nanopores poses a greater theoretical challenge. As the pore diameter is decreased, one would expect a crossover from bulk to quasi-one-dimensional behavior, which is beyond the scope of a theory based on a square-box geometry.[77] Finally, as the pore diameter is decreased, the relative fraction of water molecules in contact with the surface of the nanopore increase, and hence the contribution of surface interactions also increases. A more sophisticated physical picture should account for all of these features.

The results, presented in this work, are certainly not the last word on the thermodynamic description of the anomalies in supercooled water. Our analysis focuses on the physical susceptibilities (the second derivatives of the Gibbs energy), which demonstrate striking anomalies in the supercooled region. There is a lot of work to be done, in particular, on the comprehensive and accurate description of the molar volume and entropy, the first derivatives of the Gibbs energy, in a broad range of temperatures and pressures. This task would require a more detailed look at "non-scaling" backgrounds of thermodynamic properties and needs to account for nonasymptotic features in the scaling equation of state.

In our analysis we assume that the liquid−liquid critical point in water does exist. Although we consider this scenario to be the most plausible, other interpretations of the anomalies in supercooled water are still worth attention. In particular, recent experiments in confined water[43] may suggest a second-order phase transition line or a weakly first-order transition line replacing what is commonly interpreted as the Widom line. Such an interpretation would be more radical than any of the scenarios suggested for supercooled water thus far because it requires the existence of a vector-like order parameter similar to that in the superfluid liquid helium. Only further, more accurate, experiments and more sophisticated simulations on supercooled water can give more definite answers to these questions.

APPENDIX A: PHYSICAL SUSCEPTIBILITIES IN REVISED SCALING

The most general set of linear relations between the scaling and physical fields is given by

$$h_1 = a_1\Delta\hat{\mu} + a_2\Delta\hat{T} \tag{64}$$

$$h_2 = b_1\Delta\hat{T} + b_2\Delta\hat{\mu} \tag{65}$$

$$h_3 = \Delta\hat{P} - \Delta\hat{\mu} - \hat{s}_c\Delta\hat{T} \tag{66}$$

On the basis of these tranformations, the critical parts of the physical response functions are found through relations to be

$$(\hat{\rho}^2\hat{\kappa}_T)_{cr} = {a_1}^2\chi_1 + 2a_1b_2\chi_{12} + {b_2}^2\chi_2 \tag{67}$$

$$(\hat{\rho}\hat{\alpha}_P)_{cr} = -[a_1a_2\chi_1 + (a_1b_1 + a_2b_2)\chi_{12} + b_1b_2\chi_2] + \hat{S}(\hat{\rho}^2\hat{\kappa}_T)_{cr} \tag{68}$$

$$\left(\hat{\rho}\,\frac{\hat{C}_P}{\hat{T}}\right)_{cr} = {a_2}^2\chi_1 + 2a_2b_1\chi_{12} + {b_1}^2\chi_2 + 2\hat{S}(\hat{\rho}\hat{\alpha}_P)_{cr} - \hat{S}^2(\hat{\rho}^2\hat{\kappa}_T)_{cr} \tag{69}$$

where the reduced molar entropy $\hat{S} = (\hat{s}_c + b_1\varphi_2 + a_2\varphi_1)/(1 + a_1\varphi_1 + b_2\varphi_2)$. The revised scaling results for the lattice gas are recovered in the limit $a_1 \to 1$, $b_1 \to 1$, $b_2 \to 0$, whereas the lattice liquid, with asymmetry, corresponds to $a_2 \to 1$, $b_2 \to -1$ while a_2 represents a finite $\mu-T$ slope of the liquid−liquid transition line. In previous derivations of the response functions,[33,38] the terms proportional to $\hat{S}$ have been neglected. These terms may produce relevant singular contributions such as

$$\varphi_1\chi_1 \sim |h_2|^{\beta-\gamma} \tag{70}$$

which diverges ($\beta - \gamma \simeq -0.91$) more strongly than χ_2.

APPENDIX B: COMPARISON OF LATTICE GAS AND LATTICE LIQUID

The characteristic properties of the lattice gas are expressed in zero ordering field ($\Delta\hat{\mu} = 0$) as power laws of the reduced temperature $\Delta\hat{T}$. As follows from eq 4 and 5, the densities are given by

$$\Delta\hat{\rho} = \pm B_0|\Delta\hat{T}|^{\beta} \qquad (\Delta\hat{T} < 0) \tag{71}$$

$$\Delta\hat{s} = \frac{A_0^{\pm}}{1-\alpha}|\Delta\hat{T}|^{1-\alpha} \tag{72}$$

and the critical parts of the response functions are given by

$$(\hat{\rho}^2\hat{\kappa}_T)_{cr} = \Gamma_0^{\pm}|\Delta\hat{T}|^{-\gamma} \tag{73}$$

$$(\hat{\rho}\hat{\alpha}_P)_{cr} = \begin{pmatrix} 0 & \Delta T > 0 \\ \beta B_0|\Delta\hat{T}|^{\beta-1} & \Delta T < 0 \end{pmatrix} \tag{74}$$

$$\left(\frac{\hat{\rho}\hat{C}_P}{\hat{T}}\right)_{cr} = A_0^{\pm}|\Delta\hat{T}|^{-\alpha} \tag{75}$$

In contrast, along the same thermodynamic path ($\Delta\hat{\mu} = 0$), the densities of the lattice liquid behave as

$$\Delta\hat{\rho} \sim |\Delta\hat{T}|^{(1-\alpha)/(\beta+\gamma)} \quad (76)$$

$$\Delta\hat{s} \sim \mathrm{sgn}(\Delta\hat{T})|\Delta\hat{T}|^{\beta/(\beta+\gamma)} \quad (77)$$

where $(1-\alpha)/(\beta+\gamma) \simeq 0.57$ amd $\beta/(\beta+\gamma) \simeq 0.21$, and the response functions behave as

$$(\hat{\rho}^2\hat{\kappa}_T)_{cr} \sim |\Delta\hat{T}|^{-\alpha/(\beta+\gamma)} \quad (78)$$

$$(\hat{\rho}\hat{\alpha}_P)_{cr} \sim -\mathrm{sgn}(\Delta\hat{T})|\Delta\hat{T}|^{-(1-\beta)/(\beta+\gamma)} \quad (79)$$

$$\left(\frac{\hat{\rho}\hat{C}_p}{\hat{T}}\right)_{cr} \sim |\Delta\hat{T}|^{-\gamma/(\beta+\gamma)} \quad (80)$$

with $\alpha/(\beta+\gamma) \simeq 0.07$, $(1-\beta)/(\beta+\gamma) \simeq 0.43$ and $\gamma/(\beta+\gamma) \simeq 0.79$. Thus, below the critical point, a lattice liquid with an infinite slope of the liquid−liquid transition line in the $P-T$ plane separates into two coexisting phases with different entropy densities but with the same molecular density.

APPENDIX C: LANDAU EXPANSION FOR THE LATTICE LIQUID

In the mean-field approximation, the critical part of the field-dependent thermodynamic potential is given by a Landau expansion:[64]

$$h_3 = h_1\varphi_1 - \frac{1}{2}a_0h_2{\varphi_1}^2 - \frac{u_0}{4!}{\varphi_1}^4 \quad (81)$$

where a_0 and u_0 are constants. For simplicity, we will adopt the lattice-gas value $a_0 = 1$ while keeping the coupling constant u_0 system-dependent. In the purely symmetric lattice liquid, $a' = 0$, $\varphi_1 = \Delta\hat{s}$,

$$\Delta\hat{T} = h_1 = h_2\varphi_1 + \frac{u_0}{6}(\varphi_1)^3 = -\Delta\hat{\mu}\Delta\hat{s} + \frac{u_0}{6}(\Delta\hat{s})^3 \quad (82)$$

and

$$\Delta\hat{\rho} = -\varphi_2 = (1/2)(\Delta\varphi_1)^2 = \frac{1}{2}(\Delta\hat{s})^2 \quad (83)$$

By using the Legendre transformation $\psi(h_1,\varphi_2) = h_2\varphi_2 - h_3$ and eq 83, we obtain the critical part of the Helmholtz-energy density $\psi(\Delta\hat{\rho},\Delta\hat{T}) = \psi(\varphi_2,h_1)$ in terms of molecular density and temperature:

$$\psi(\Delta\hat{\rho},\Delta\hat{T}) = \sqrt{2}\Delta\hat{T}(\Delta\hat{\rho})^{1/2} + \frac{u_0}{6}(\Delta\hat{\rho})^2 \quad (84)$$

The chemical potential diverges at the critical isochor for any finite $\Delta\hat{T}$:

$$\Delta\hat{\mu} = \frac{\sqrt{2}}{2}\Delta\hat{T}|\Delta\hat{\rho}|^{-1/2} + \frac{u_0}{6}|\Delta\hat{\rho}| \quad (85)$$

However, the density derivative of the chemical potential,

$$\left(\frac{\partial\hat{\mu}}{\partial\hat{\rho}}\right)_T = -\frac{\sqrt{2}}{4}\Delta\hat{T}|\Delta\hat{\rho}|^{-3/2} + \frac{u_0}{6} \quad (86)$$

vanishes at the critical point satisfying

$$\Delta\hat{T} = \frac{2u_0}{3\sqrt{2}}|\Delta\hat{\rho}|^{3/2} \quad (87)$$

Finally, if the liquid−liquid transition line has a finite $P-T$ slope, we obtain

$$\Delta\hat{\rho} = \frac{1}{2}(\Delta\hat{s})^2 + a'\Delta\hat{s} \quad (88)$$

and

$$\psi(\Delta\hat{\rho},\Delta\hat{T}) = \sqrt{2}\Delta\hat{T}|\Delta\hat{\rho}|^{1/2} + \frac{u_0}{6}|\Delta\hat{\rho}|^2 - a'\Delta\hat{T} + a'\frac{u_0}{2\sqrt{2}}\Delta\hat{\rho}^{3/2} \quad (89)$$

In contrast to the Landau expansion for the lattice gas, there are fractional powers of the reduced density in expansion of the lattice-liquid Helmholtz energy.

AUTHOR INFORMATION

Corresponding Author

*E-mail: anisimov@umd.edu.

ACKNOWLEDGMENT

We thank F. Mallamace and E. Tombari for sending us their experimental data on water in the supercooled region. We appreciate fruitful discussions with C. A. Angell, P. G. Debenedetti, A. Faraone, O. Mishima, and C. M. Sorensen and acknowledge collaboration with members of our research group, namely, D. A. Fuentevilla, V. Holten, J. Kalova, and J. V. Sengers. M.A.A. enjoyed many encouraging interactions with the attendees of the HES70 Symposium "Horizons in Emergence & Scaling". This research was supported by the Division of Chemistry of the National Science Foundation (Grant No. CHE-1012052).

REFERENCES

(1) Voronel, A. V. *JETP Lett.* **1971**, *14*, 174–177.
(2) Voronel, A. V. In *Phase Transitions and Critical Phenomena*; Domb, C., Green, M. S., Eds.; Academic Press: London, 1976; Vol. 5B, pp 343−391.
(3) Anisimov, M. A.; Voronel, A. V.; Zaugol'nikova, N. S.; Ovodov, G. I. *JETP Lett.* **1972**, *15*, 317–319.
(4) Angell, C. A.; Shuppert, J.; Tucker, J. C. *J. Phys. Chem.* **1973**, *77*, 3092–3099.
(5) Rasmussen, D. H.; MacKenzie, A. P. *J. Chem. Phys.* **1973**, *59*, 5003–5013.
(6) Oguni, M.; Angell, C. A. *J. Chem. Phys.* **1980**, *73*, 1948–1954.
(7) Angell, C. A.; Oguni, M.; Sichina, W. J. *J. Phys. Chem.* **1982**, *86*, 998–1002.
(8) Kanno, H.; Angell, C. A. *J. Chem. Phys.* **1979**, *70*, 4008–4016.
(9) Speedy, R. J.; Angell, C. A. *J. Chem. Phys.* **1976**, *65*, 851–858.
(10) Hare, D. E.; Sorensen, C. M. *J. Chem. Phys.* **1986**, *84*, 5085–5089.
(11) Hare, D. E.; Sorensen, C. M. *J. Chem. Phys.* **1987**, *87*, 4840–4845.
(12) Poole, P. H.; Sciortino, F.; Essmann, U.; Stanley, H. E. *Nature* **1992**, *360*, 324–328.
(13) Stanley, H. E.; Angell, C. A.; Essmann, U.; Hemmati, M.; Poole, P. H.; Sciortino, F. *Physica A* **1994**, *205*, 122–139.
(14) Tanaka, H. *J. Chem. Phys.* **1996**, *105*, 5099–5111.
(15) Tanaka, H. *Nature* **1996**, *380*, 328–330.
(16) Harrington, S.; Poole, P. H.; Sciortino, F.; Stanley, H. E . *J. Chem. Phys.* **1997**, *107*, 7443–7450.

(17) Yamada, M.; Mossa, S.; Stanley, H. E.; Sciortino, F. *Phys. Rev. Lett.* **2002**, *88*, 195701/1–195701/4.
(18) Paschek, D. *Phys. Rev. Lett.* **2005**, *94*, 217802/1–217802/4.
(19) Jedlovszky, P.; Vallauri, R. *J. Chem. Phys.* **2005**, *122*, 081101/1–081101/4.
(20) Paschek, D.; Rueppert, A.; Geiger, A. *ChemPhysChem* **2008**, *9*, 2737–2741.
(21) Liu, Y.; Panagiotopoulos, A. Z.; Debenedetti, P. G. *J. Chem. Phys.* **2009**, *131*, 104508/1–104508/7.
(22) Abascal, J. L. F.; Vega, C. *J. Chem. Phys.* **2010**, *133*, 234502/1–234502/8.
(23) Poole, P. H.; Sciortino, F.; Grande, T.; Stanley, H. E.; Angell, C. A. *Phys. Rev. Lett.* **1994**, *73*, 1632–1635.
(24) Truskett, T. M.; Debenedetti, P. G.; Sastry, S.; Torquato, S. *J. Chem. Phys.* **1999**, *111*, 2647–2656.
(25) Lee, H. K.; Swendsen, R. H. *Phys. Rev. B* **2001**, *64*, 214102/1–214102/5.
(26) Truskett, T. M.; Dill, K. A. *J. Phys. Chem. B* **2002**, *106*, 11829–11842.
(27) Girardi, M.; Balladares, A. L.; Henriques, V. B.; Barbosa, M. C. *J. Chem. Phys.* **2007**, *126*, 064503/1–064503/6.
(28) Stokely, K.; Mazza, M. G.; Stanley, H. E.; Franzese, G. *Proc. Natl. Acad. Sci. U. S. A.* **2010**, *107*, 1301–1306.
(29) Mishima, O.; Stanley, H. E. *Nature* **1998**, *392*, 164–168.
(30) Mishima, O. *Phys. Rev. Lett.* **2000**, *85*, 334–336.
(31) Mishima, O. *J. Chem. Phys.* **2005**, *123*, 154506/1–154506/4.
(32) Mishima, O. *J. Chem. Phys.* **2010**, *133*, 144503/1–144503/6.
(33) Fuentevilla, D. A. A Scaled Parametric Equation of State for the Liquid-Liquid Critical Point in Supercooled Water. *M.S. Thesis*, University of Maryland, College Park, MD, 2007.
(34) Speedy, R. *J. Phys. Chem.* **1982**, *86*, 3002–3005.
(35) Sastry, S.; Debenedetti, P. G.; Sciortino, F.; Stanley, H. E. *Phys. Rev. E* **1996**, *53*, 6144–6154.
(36) Rebelo, L. P. N.; Debenedetti, P. G.; Sastry, S. *J. Chem. Phys.* **1998**, *109*, 626–633.
(37) Angell, C. A. *Science* **2008**, *319*, 582–587.
(38) Fuentevilla, D. A.; Anisimov, M. A. *Phys. Rev. Lett.* **2006**, *97*, 195702/1–195702/4. Fuentevilla, D. A.; Anisimov, M. A. *Phys. Rev. Lett.* **2007**, *98*, 149904/1.
(39) Wagner, W.; Pruss, A. *J. Phys. Chem. Ref. Data* **2002**, *31*, 387–535.
(40) Liu, L.; Chen, S.-H.; Faraone, A.; Yen, C.-W.; Mou, C.-Y. *Phys. Rev. Lett.* **2005**, *95*, 117802/1–117802/4.
(41) Mallamace, F.; Corsaro, C.; Broccio, M.; Branca, C.; González-Segredo, N.; Spooren, J.; Chen, S.-H.; Stanley, H. E. *Proc. Natl. Acad. Sci. U. S. A.* **2008**, *105*, 12725–12729.
(42) Mallamace, F. *Proc. Natl. Acad. Sci. U. S. A.* **2009**, *106*, 15097–15098.
(43) Zhang, Y.; Faraone, A.; Kamitakahara, W. A.; Liu, K.-H.; Mou, C.-Y.; Leão, J. B.; Chang, S.; Chen, S.-H. *arXiv*:1005.5387v2 [cond-mat.soft], 2010.
(44) Nagoe, A.; Kanke, Y.; Oguni, M.; Namba, S. *J. Phys. Chem. B* **2010**, *114*, 13940–13943.
(45) Lee, T. D.; Yang, C. N. *Phys. Rev.* **1952**, *87*, 410–419.
(46) Fisher, M. E. In *Lecture notes in Physics*; Hahne, F. J. W., Ed.; Springer: Berlin, 1982; Vol. 186, pp 1−139.
(47) Sengers, J. V.; Shanks, J. G. *J. Stat. Phys.* **2009**, *137*, 857–877.
(48) Guida, R.; Zinn-Justin, J. *J. Phys. A* **1998**, *31*, 8103–8121.
(49) Behnejad, H.; Sengers, J. V.; Anisimov, M. A. In *Applied Thermodynamics of Fluids*; Goodwin, A., Sengers, J. V., Peters, C. J., Eds.; IUPAC, RSC Publishing: Cambridge, U.K., 2010; pp 321−366.
(50) Anisimov, M. A.; Agayan, V. A.; Collings, P. J. *Phys. Rev. E* **1998**, *57*, 582–595.
(51) Fisher, M. E.; Zinn, S.-Y. *J. Phys. A* **1998**, *31*, L629–L635.
(52) Fisher, M. E.; Orkoulas, G. *Phys. Rev. Lett.* **2000**, *85*, 696–699.
(53) Kim, Y. C.; Fisher, M. E.; Orkoulas, G. *Phys. Rev. E* **2003**, *67*, 061506/1–061506/21.
(54) Anisimov, M. A.; Wang, J. T. *Phys. Rev. Lett.* **2006**, *97*, 025703/1–025703/4.
(55) Wang, J.; Anisimov, M. A. *Phys. Rev. E* **2007**, *75*, 051107/1–051107/19.
(56) Sengers, J. V.; Levelt Sengers, J. M. H. In *Progress in Liquid Physics*; Croxton, C. A., Ed.; Wiley: Chichester, U. K., 1978; pp 103−174.
(57) Davis, C. M., Jr.; Litovitz, T. A. *J. Chem. Phys.* **1965**, *42*, 2563–2576.
(58) Vedamuthu, V.; Singh, S.; Robinson, G. W. *J. Phys. Chem.* **1994**, *98*, 2222–2230.
(59) Röntgen, W. C. *Ann. Phys. (Leipzig)* **1892**, *281*, 91–97.
(60) Ponyatovskii, E. G.; Sinand, V. V.; Pozdnyakova, T. A. *JETP Lett.* **1994**, *60*, 360–364.
(61) Moynihan, C. T. *Mater. Res. Soc. Symp. Proc.* **1997**, *455*, 411–425.
(62) Angell, C. A. *J. Phys. Chem.* **1971**, *75*, 3698–3705.
(63) Levelt Sengers, J. M. H. *Physica A* **1979**, *98*, 363–402.
(64) Landau, L. D.; Lifshitz, E. M. *Statistical Physics*, 3rd ed.; Sykes, J. B.;, Kearsley, M. J., translators; Butterworth Heinemann: Oxford, U.K., 1980; Part 1.
(65) Prigogine, I.; Defay, R. *Chemical Thermdynamics*; Longmans, Green & Co.: London, 1954.
(66) Schofield, P. *Phys. Rev. Lett.* **1969**, *22*, 606–608.
(67) Brézin, E.; Wallace, D. J.; Wilson, K. G. *Phys. Rev. Lett.* **1972**, *29*, 591–594.
(68) Wallace, D. J.; Zia, R. K. P. *J. Phys. C* **1974**, *7*, 3480–3490.
(69) Kim, Y. C.; Anisimov, M. A.; Sengers, J. V.; Luijten, E. *J. Stat. Phys.* **2003**, *110*, 591–609.
(70) Archer, D. G.; Carter, R. W. *J. Phys. Chem. B* **2000**, *104*, 8563–8584.
(71) Tombari, E.; Ferrari, C.; Salvetti, G. *Chem. Phys. Lett.* **1999**, *300*, 749–751.
(72) Kalova, J. Unpublished work.
(73) Ito, K.; Moynihan, C. T.; Angell, C. A. *Nature* **1999**, *398*, 492–495.
(74) Fisher, M. E.; Barber, M. N. *Phys. Rev. Lett.* **1972**, *28*, 1516–1519.
(75) Huang, C.; Weiss, T. M.; Nordlund, D.; Wikfeldt, K. T.; Pettersson, L. G. M.; Nilsson, A. *J. Chem. Phys.* **2010**, *133*, 134504/1–134504/5.
(76) Privman, V.; Fisher, M. E. *Phys. Rev. B* **1984**, *30*, 322–327.
(77) Rudnick, J.; Guo, H.; Jasnow, D. *J. Stat. Phys.* **1985**, *41*, 353–373.
(78) Esser, A.; Dohm, V.; Chen, X. S. *Physica A* **1995**, *222*, 355–397.
(79) Voronov, V. P.; Buleko, V. M. *JETP* **1998**, *86*, 586–590.
(80) Chen, X. S.; Dohm, V.; Talapov, A. L. *Physica A* **1996**, *232*, 375–396.